

## Long-Range Signal Transmission in Autocrine Relays

Michal Přibyl,\* Cyrill B. Muratov,<sup>†</sup> and Stanislav Y. Shvartsman\*

\*Department of Chemical Engineering and Lewis-Sigler Institute for Integrative Genomics, Princeton University Princeton, New Jersey; and

<sup>†</sup>Department of Mathematical Sciences and Center for Applied Mathematics and Statistics, New Jersey Institute of Technology, Newark, New Jersey

**ABSTRACT** Intracellular signaling induced by peptide growth factors can stimulate secretion of these molecules into the extracellular medium. In autocrine and paracrine networks, this can establish a positive feedback loop between ligand binding and ligand release. When coupled to intercellular communication by autocrine ligands, this positive feedback can generate constant-speed traveling waves. To demonstrate that, we propose a mechanistic model of autocrine relay systems. The model is relevant to the physiology of epithelial layers and to a number of in vitro experimental formats. Using asymptotic and numerical tools, we find that traveling waves in autocrine relays exist and have a number of unusual properties, such as an optimal ligand binding strength necessary for the maximal speed of propagation. We compare our results to recent observations of autocrine and paracrine systems and discuss the steps toward experimental tests of our predictions.

### INTRODUCTION

The versatility of cell-cell communication relies on sophisticated modules for signal generation, transmission, detection, and processing (Hunter, 2000; Jordan et al., 2000). Compared to signal detection and intracellular transduction, signal generation and transmission are relatively poorly understood. For instance, even though the Epidermal Growth Factor Receptor (EGFR) signaling network has been studied over the past four decades, the molecules that mediate the release of EGFR ligands are being identified only now (Schlessinger, 2000; Lee et al., 2001; Merlos-Suarez et al., 2001; Sunnarborg et al., 2002; Yan et al., 2002). Current work on regulated ligand release focuses on the identification of the relevant molecules and intracellular events. At the same time, it is important to understand how these processes operate in tissues.

Many growth factors and cytokines are released by intracellular or cell surface proteases (Dello and Rovida, 2002). In a number of developmental and physiological contexts, receptors are in excess and their activation is regulated by ligand release and delivery (Freeman and Gurdon, 2002; Kheradmand and Werb, 2002). The availability and activity of ligand-releasing enzymes can be regulated both intra- and extracellularly. Notably, the ligand-releasing enzymes can be activated by the signaling pathways that are stimulated by the ligands they release. Therefore, a positive feedback loop can be established in the regime when the producing cell effectively recaptures and responds to the secreted ligand (Carpenter, 1999; Gschwind et al., 2001; Dello and Rovida, 2002). Such feedback from ligand binding to ligand release is a frequent

component of autocrine and paracrine EGFR networks (Dent et al., 1999; Fan and Derynck, 1999; Gechtman et al., 1999; Freeman, 2000; Chen et al., 2001).

Intracellular signaling by the Ras-MAPK pathway can mediate positive feedback in the EGFR system, Fig. 1. In *Drosophila*, MAPK activated by EGFR induces the transcription of Rhomboid, an intracellular protease, that processes Spitz, a secreted EGFR ligand (Mantova and Hsu, 1998; Sapir et al., 1998; Wasserman and Freeman, 1998; Guichard et al., 1999; Bang and Kintner, 2000; Hsu et al., 2001; Lee et al., 2001), Fig. 1 *A*. In mammalian EGFR systems, MAPK can activate the cell-surface ligand-releasing proteases, such as TACE and Kuzbanian (Fan and Derynck, 1999; Merlos-Suarez and Arribas, 1999; Doedens and Black, 2000; Montero et al., 2000, 2002; Merlos-Suarez et al., 2001; Diaz-Rodriguez et al., 2002), Fig. 1 *B*. The MAPK-mediated feedback in the EGFR system is important in a number of developmental and clinical contexts. The EGFR/MAPK/Rhomboid/Spitz feedback functions throughout the fruit fly development (Casci and Freeman, 1999). The EGFR/MAPK/TACE/TGF $\alpha$  network can protect cells against ionizing radiation and prevent the success of cancer radiotherapy (Hagan et al., 2000; Harari and Huang, 2001). These feedbacks rely on the regulation of production and/or activity of ligand-releasing enzymes; other mechanisms relying on the induction of receptor or its ligands have also been described (Doraiswamy et al., 2000; Albanell et al., 2001).

Here, we report a model-based analysis of cell communication in epithelial layers equipped with autocrine positive feedback loops. Our main interest is the mechanisms of signal transmission in autocrine systems. Consider a two-dimensional layer of cells covered by a medium where a soluble ligand can diffuse, Fig. 1 *C*. The upper boundary of the medium is impermeable to the ligand. The lower boundary, formed by the cellular layer, can reversibly bind the secreted ligand. The ligand-receptor complexes on the cell surfaces stimulate the intracellular processes leading

Submitted September 17, 2002, and accepted for publication November 12, 2002.

Address reprint requests to Stanislav Y. Shvartsman, Dept. of Chemical Engineering and Lewis-Sigler Institute for Integrative Genomics, Princeton University, Princeton, NJ 08544. Tel.: 609-258-4694; Fax: 609-258-0211; E-mail: stas@princeton.edu.

© 2003 by the Biophysical Society

0006-3495/03/02/883/14 \$2.00

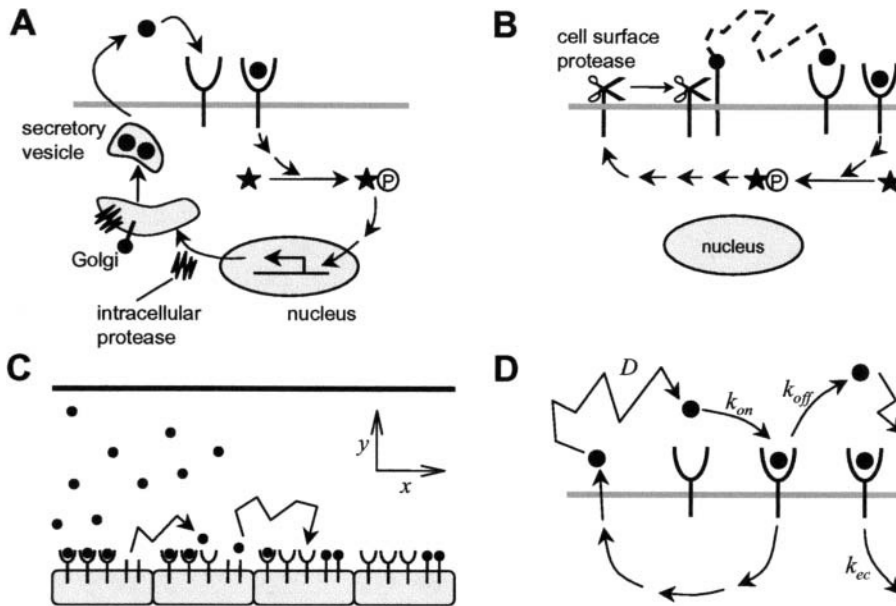


**FIGURE 1** Positive feedback in autocrine systems. (A) Positive feedback relying on transcription. Intracellular signaling activated by autocrine ligands induces and maintains the transcription of the ligand-releasing enzyme. (B) The feedback is mediated by the activation of the ligand-releasing enzyme. (C) The geometry of cell communication in the model of an autocrine relay. Ligand is diffusing in extracellular medium above the cellular layer. (D) Receptor-mediated processes in the model: ligand release, extracellular transport, reversible binding, and endocytosis.  $D$ , ligand diffusivity;  $k_{on}$ , ligand-receptor association constant;  $k_{off}$ , complex dissociation constant; and  $k_{ec}$ , ligand-induced internalization rate constant.

to further ligand release, Fig. 1 *D*. Imagine a quiescent epithelial layer, in which ligand release is in the “off” state, Fig. 1 *C*. A localized stimulation of the cellular layer creates a localized source of ligand. As a result, receptor occupancy and, potentially, ligand release would increase in the neighboring cells. Will this excitation spread across the layer? If yes, then how is the speed of signal transmission in such an autocrine relay related to the parameters in the modules for ligand release, binding, transport, and signaling? A mechanistic model of ligand release and transport can provide a systematic framework for addressing these questions.

A few words on the considered geometry of cell communication. In vitro, this geometry can be realized within the cell and tissue culture assays, where an epithelial layer or a confluent monolayer of autocrine cells is covered by liquid medium; the experimentalist controls the height of the medium (Mandell et al., 2001). This arrangement is also realized in a number of developmental contexts. For example, in *Drosophila* egg development, a layer of epithelial follicle cells covers a large oocyte (Spradling, 1993; Dobens and Raftery, 2000). Both the oocyte and the follicle cells secrete the EGFR ligands, but EGFR is expressed only in the follicle cells. Hence, ligand diffuses in the gap between the reflective and the receptor-covered surfaces; the size of this gap is less than one micron.

The paper is organized as follows. In the next section we present a model for ligand release, transport, and signaling. We analyze the model using a combination of analytical and computational tools. First, we solve the simplified version of the model in the regime when receptors are in excess and ligand release obeys simple threshold-like kinetics. These assumptions are relaxed during the computational analysis of the model. We conclude with the outline of future directions

for modeling and suggest experimental tests of our predictions.

## MODEL FORMULATION

### Equations and scaling

We consider an infinite layer of cells covered by an extracellular medium of height  $h$ . The model describes the coupled dynamics of secreted ligands ( $S$ ), surface receptors ( $R$ ), ligand-receptor complexes ( $C$ ), and ligand-releasing proteases ( $P$ ). The ligand reversibly binds to cell surface receptors; the ligand-receptor complex is degraded through the combination of complex dissociation and receptor-mediated endocytosis. Let us define the ligand concentration at the cellular layer as  $\bar{S}(x, t) \equiv S(x, 0, t)$ .  $Q_r$  is the rate of receptor synthesis;  $g_p$  and  $g_r$  denote the linear gains in the protease and ligand production, respectively. The balance equations and the corresponding boundary conditions take the following form:

$$\frac{\partial S}{\partial t} = D \left( \frac{\partial^2 S}{\partial x^2} + \frac{\partial^2 S}{\partial y^2} \right), \quad (1)$$

$$\frac{\partial R}{\partial t} = -k_{on} R \bar{S} + k_{off} C - k_{ec} R + Q_r, \quad (2)$$

$$\frac{\partial C}{\partial t} = k_{on} R \bar{S} - (k_{off} + k_{ec}) C, \quad (3)$$

$$\frac{\partial P}{\partial t} = -k_p P + g_p \sigma(C), \quad (4)$$

$$\left( D \frac{\partial S}{\partial y} - k_{on} R \bar{S} \right) \Big|_{y=0} = -k_{off} C - g_r P \quad \frac{\partial S}{\partial y} \Big|_{y=h} = 0, \quad (5)$$

where  $t$  is time,  $x$  is the spatial coordinate parallel to the cellular layer, and  $y$  is the spatial coordinate perpendicular to it (see Fig. 1 *C*).

The boundary conditions at the surface of the cellular layer account for diffusive flux of extracellular ligand, reversible ligand-receptor binding, and

generation by intracellular or cell surface ligand-releasing proteases. In our model, ligand generation is controlled by the activity of the protease and has zero order with respect to the amount of cell-associated ligand precursor. In other words, the cell-associated ligand precursor is in excess and is not significantly depleted by the proteolytic release. This is true in at least two experimental EGFR systems: Spitz release by Rhomboid in *Drosophila* development (Rutledge et al., 1992; Freeman, 1997; Stemerink and Jacobs, 1997; Stevens, 1998; Wasserman and Freeman, 1998; Bang and Kintner, 2000) and release of TGF $\alpha$  from autocrine epidermoid carcinoma cells (Dent et al., 1999).

In the present formulation of the model, ligand-receptor complex is internalized in the first-order process with rate constant  $k_{ec}$ . A straightforward extension of the model can account for the following processes of ligand/receptor trafficking. This will require introduction of additional state variables corresponding to species at various stages of endocytic cycle (Burke et al., 2001; Waterman and Yarden, 2001). The parameters of the model and their typical values are listed in Table 1.

The production of the ligand-releasing protease,  $\sigma(C)$ , is described by the sigmoidal function of the number of occupied receptors. This sigmoidal dependence can arise from the true cooperativity in ligand release and/or from the composition of the intermediate steps between ligand/receptor binding and protease activation; see Ferrell and Xiong (2001) for the discussion of mechanisms that generate sharp thresholds through a combination of multiple steps in cascades of enzymatic reactions. For simplicity, we assume that, once internalized, the ligand-receptor complex is "lost" for signaling. This is true for the ligands that quickly dissociate from receptors in endosomes, such as TGF $\alpha$  (Haugh et al., 1999). Other ligands, such as EGF, stay associated with receptor and might signal from the endosomes (Haugh et al., 1999; Schoeberl et al., 2002). Signaling from endosomes prolongs the duration of receptor-mediated ERK2 activation (Wong et al., 2002); hence, it is expected to promote nonlinear effects mediated by positive feedback loops.

We assume that protease synthesis (or activation) is an algebraic function of the number of ligand-receptor complexes. The nonlinearity  $\sigma(C)$  combines a large number of processes leading from receptor binding to protease generation. This simple model assumes that these steps are fast, and that protease generation can instantaneously follow the number of occupied receptors. At this stage, we need this assumption to advance our analysis. Toward the end of the paper, we discuss and computationally analyze the potential role of a time lag between receptor occupancy and receptor activation (Fig. 8 B). In the simplest case, this lag can be parameterized by a constant time delay. This would modify the right-hand side of Eq. 4 (the

sigmoidal function would depend on the number of complexes at a previous moment in time:  $\sigma(C(t - t_D))$ ). In terms of the standard control theory, the model for protease dynamics is then classified as a first-order system with delay (Ogunnaike and Ray, 1994).

The model is rendered dimensionless by the following transformations:

$$\tau \equiv tk_p, \quad \zeta \equiv x/L_x, \quad \eta \equiv y/h, \quad s \equiv S/S_0, \quad (6)$$

$$c \equiv C/C_0, \quad p \equiv P/P_0, \quad r \equiv R/R_0,$$

where

$$S_0 = (k_{off} + k_{ec})(g_r g_p k_{er}) / (k_p k_{on} k_{ec} Q_r), \quad C_0 = (g_r g_p) / (k_p k_{ec}),$$

$$P_0 = g_p / k_p, \quad R_0 = Q_r / k_{er}, \quad L_x = (D k_{er}) / (k_{on} Q_r) \quad (7)$$

The time scale is set by the dynamics of protease degradation. The vertical length scale is scaled by the height of the medium. The horizontal length scale is derived from the previous analysis of the spatial extent of autocrine loops. Specifically, the length scale  $L_x$  appears in the expressions for the cumulative distribution functions that characterize the extrema of random trajectories followed by ligands diffusing above the receptor-covered plane (Shvartsman et al., 2001).

After rescaling, we get:

$$\tau_s \frac{\partial s}{\partial \tau} = \frac{\partial^2 s}{\partial \zeta^2} + \frac{1}{\alpha^2} \frac{\partial^2 s}{\partial \eta^2}, \quad (8)$$

$$\tau_r \frac{\partial r}{\partial \tau} = -\gamma(r\bar{s} - (1 - \beta)c) - r + 1, \quad (9)$$

$$\tau_c \frac{\partial c}{\partial \tau} = r\bar{s} - c, \quad (10)$$

$$\frac{\partial p}{\partial \tau} = -p + \sigma(c), \quad (11)$$

$$\left( \frac{\partial s}{\partial \eta} - \alpha r s \right) \Big|_{\eta=0} = -\alpha((1 - \beta)c + \beta p) \quad \frac{\partial s}{\partial \eta} \Big|_{\eta=1} = 0. \quad (12)$$

There are six dimensionless parameters in the rescaled model:

$$\alpha = k_{on} R_0 h / D \quad \beta = k_{ec} / (k_{off} + k_{ec}) \quad \gamma = g_r g_p / (k_p Q_r \beta)$$

$$\tau_s = k_p D / (k_{on} R_0)^2 \quad \tau_c = k_p / (k_{off} + k_{ec}) \quad \tau_r = k_p / k_{er} \quad (13)$$

The first of these,  $\alpha$ , is the Damköhler number that characterizes the relative rates of diffusion and binding (Deen, 1998). Note that  $\alpha$  is also the ratio of the geometric and dynamic length scales,  $h$  and  $L_x$ , respectively. The second dimensionless group,  $\beta$ , characterizes the relative rates of endocytosis and dissociation;  $\gamma$  is proportional to the ratio of the ligand and receptor generation rates (i.e., ratio of  $g_r g_p / k_p$  and  $Q_r$ );  $\tau_s$ ,  $\tau_r$ , and  $\tau_c$  characterize the relative time scales of the extracellular ligand, and of the free and bound receptors, respectively.

## Steady-state multiplicity and traveling fronts

The spatially uniform steady states of Eqs. 8–12 satisfy:

$$c - \sigma(c) = 0, \quad r = 1 - \beta\gamma c, \quad p = \sigma(c), \quad s = c / (1 - \beta\gamma c). \quad (14)$$

**TABLE 1** Parameters of the model

Parameter	Description	Range
$D$	Ligand diffusivity	$10^{-8} - 10^{-6} \text{ cm}^2/\text{s}$
$h$	Height of the extracellular medium	$10 \text{ } \mu\text{m} - 1000 \text{ } \mu\text{m}$
$k_{ec}$	Ligand-induced internalization rate constant	$0.1 - 0.3 \text{ min}^{-1}$
$k_{er}$	Constitutive internalization rate constant	$0.01 - 0.1 \text{ min}^{-1}$
$k_{on}$	Receptor/ligand association constant	$1 - 1 \times 10^3 \text{ } \mu\text{M}^{-1} \text{ min}^{-1}$
$k_p$	Protease degradation rate constant	$0.01 - 0.03 \text{ min}^{-1}$
$K_D = k_{off}/k_{on}$	Ligand/receptor-complex equilibrium constant	$0.1 - 10 \text{ nM}$
$R_0 = Q_r/k_{er}$	Number of receptors per cell surface in absence of a ligand	$1 \times 10^3 - 1 \times 10^6 \text{ receptors/cell surface area}$

Model parameters, Lauffenburger and Linderman, 1993; Lauffenburger et al., 1995; Lauffenburger et al., 1996.

The first equation is the balance of linear and sigmoidal functions, a classical mechanism for the generation of steady state multiplicity; Fig. 2 *A* (Keener, 1998; Fall et al., 2002). Thus, depending on the parameters of the sigmoidal nonlinearity, the system of Eq. 14 may have either one or two stable steady states. In the case of bistability, the first of the steady states corresponds to the “off” state of the autocrine loop, with the zero rate of ligand release— $c = 0$ ,  $p = 0$ ,  $r = 1$ ,  $s = 0$ . The second steady state corresponds to the “on” state of the autocrine loop, with nonzero level of ligand-receptor complexes and appreciable rate of ligand release.

We study how the system switches between the two stable steady states of the autocrine loop. In particular, we look for solutions in the form of constant speed traveling fronts that connect these steady states. We analyze the dependence of the front properties on the molecular, cellular, and geometric parameters of autocrine relays.

Our main finding is that such fronts may indeed be realized in autocrine relay systems. They arise as a result of the coupling of cells by secreted autocrine ligands; this coupling is provided through the diffusion of the ligand in the extracellular space. Note that this form of coupling is different from the one that is usually encountered in models of bistable media, in which an autocatalytic substance both propagates by diffusion and undergoes the autocatalytic reaction at the same time (Mikhailov, 1994; Keener, 1998). In our model, the diffusing variable is just a messenger mediating communication within the layer of autocrine cells. The positive feedback results from the interaction between the messenger and the localized species—in our case, bound receptors and ligand-releasing proteases. Furthermore, the nature of transport in our problem makes the coupling nonlocal. A localized change in the values of nondiffusing variables affects the entire distribution of the messenger concentration.

The fronts are analyzed using a combination of analytical and computational approaches. In the computational experiments, we were starting with the autocrine layer in the “off” state and following the spatiotemporal evolution of the localized disturbance that activated the protease dynamics. We characterize the shape and speed of the traveling front that is established after the initial transient period. In the following, the description of computational experiments is preceded by the discussion of the analytical solution for the fronts in a certain limiting regime. Specifically, we consider the regime that is characterized by the fast dynamics of ligand-receptor complexes, the vast excess of empty receptors, and infinitely sharp nonlinearity of the protease production term. The analytical solution obtained in this regime enables a complete parametric analysis of the fronts and reveals a number of their unusual properties.

### Analytical solution of the simplified model

The ligand-limited regime is characterized by the small ratio of the rates of ligand release and receptor synthesis,  $\gamma \ll 1$ . In this case, the first term in the right side of Eq. 9 for the dynamics of empty receptors can be neglected. As a result, the balance for empty receptors is effectively uncoupled from other variables and the dimensionless concentration of free receptors is constant:

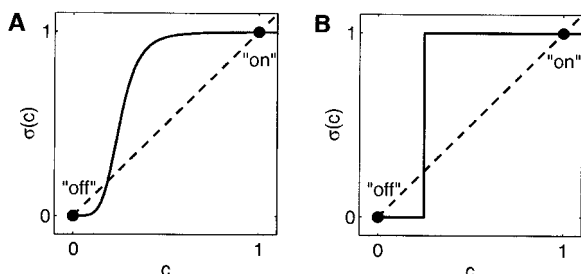


FIGURE 2 (A) Graphical solution of Equation 14, where  $\sigma(c)$  is chosen to be a Hill function  $\sigma(c) = c^n/(k^n + c^n)$ . (B) The case of the Heaviside nonlinearity:  $\sigma(c) = H(c - c_0)$ . No ligand is released in the “off” steady state. Autocrine loop is activated in the “on” steady state.

$r \approx 1$ . The magnitude of  $\gamma$  characterizes the extent to which receptor is in excess with respect to ligand (see the discussion of the dimensionless groups in the previous section), and is not explicitly related to the time scales of binding. In the large number of developmental and physiological settings, receptor is in excess and its activation is controlled by ligand availability (Freeman and Gurdon, 2002; Kheradmand and Werb, 2002; Sunnarborg et al., 2002). When receptors are in vast excess, their level is not strongly affected by the ligand-induced endocytosis and can be assumed constant across the traveling front.

When the time scale characterizing the equilibration of ligand-receptor complexes in the surface layer ( $\eta = 0$ ) is fast, and  $\tau_c \ll 1$ , these species can be eliminated using a pseudo-steady-state approximation:  $c(\zeta, \tau) = s(\zeta, 0, \tau)$ . The time scale characterizing the relaxation of ligand-receptor complexes is expected to be short compared to the time scale characterizing the protease activation. This time scale is set by the magnitude of the rate constant  $k_p$ , which determines the rate with which the protease reacts to a change in the level of its activation. For the case of Rhomboid, an intracellular ligand-releasing protease that is transcriptionally activated by the EGFR signaling (Mantrova and Hsu, 1998; Wasserman and Freeman, 1998; Urban et al., 2002), this time scale of the protease activation is definitely longer than the one for binding. In the case of TACE, a cell surface metalloprotease activated by the processes that does not rely on transcription, this assumption has to be checked experimentally (Dent et al., 1999; Gechtman et al., 1999; Dello and Rovida, 2002).

Thus, under the conditions  $\tau_c \gg 1$ ,  $\gamma \ll 1$ , the system 8–12 is reduced to the two equations for the extracellular ligand ( $s$ ), Eq. 8, and the ligand-releasing protease ( $p$ ), Eq. A1, in the Appendix. The only source of nonlinearity is provided the sigmoidal generation term in protease dynamics. A sharp sigmoidal nonlinearity can be approximated by a Heaviside function:  $\sigma(c) \approx H(c - c_0)$ , Fig. 2 *B*. In this case, the problem can be solved analytically; see Appendix. The main result is the implicit equation that links the front speed to the geometric, molecular, and cellular parameters of the autocrine loop, Eq. A18. This equation was solved graphically to produce the parametric plots in the next section.

## RESULTS AND DISCUSSION

### Fronts in the asymptotic regime

In the ligand-limited regime ( $\gamma \ll 1$ ) with fast binding ( $\tau_c \ll 1$ ) and sharp nonlinearity ( $\sigma(c) \approx H(c - c_0)$ ), the properties of propagating fronts depend on four dimensionless parameters. The value of  $c_0$  defines the threshold of the nonlinearity,  $\tau_s$  is the relative time scale for the dynamics of the extracellular ligand,  $\alpha$  compares the rates of binding and transport, and  $\beta$  depends on the kinetic parameters of the ligand-receptor complex. Given the values of these parameters, the formulas derived in the Appendix provide the spatial profile and the speed of the propagating front. Fig. 3 presents the spatial profiles of ligand and protease for a particular set of parameters corresponding to the advancing “on” state of the autocrine loop.

The molecular and cellular parameters, such as the density of cell surface receptors ( $R_0 = Q_r/K_{eq}$ ) and binding rate constant ( $k_{on}$ ), appear in several dimensionless groups; hence, their effect on the front properties is not immediately obvious. In the ligand-limited regime, the total number of receptors and the rate constant of the forward binding reaction always appear as a product,  $k_{on}R_0$ , that characterizes the rate of the forward binding reaction; this product has the dimension of velocity. The kinetic properties of the ligand-

receptor complex are combined in the dimensionless ratio of rates of dissociation and internalization:  $k_{ec}/(k_{off} + k_{ec})$ . The geometric length scale,  $h$ , appears in the Damköhler number,  $\alpha$ , that regulates the nonuniformity of solution in the vertical direction, see Eqs. 8 and 12.

Figs. 4 and 5 show the effects of molecular, cellular, and geometric parameters on the speed of the propagating solutions. We fix the diffusion coefficient and the height of the extracellular medium and analyze the effect of the binding and trafficking parameters. The height of the medium is 1 mm, a typical value encountered in cell and tissue culture assays of autocrine loops (DeWitt et al., 2001); ligand diffusivity is set to  $10^{-6} \text{ cm}^2 \text{ s}^{-1}$ , a typical value for the diffusivity of a protein in solution.

Fig. 4 *A* presents a two-parameter plot of the front speed on the rate of forward-binding reaction ( $k_{on}$  and  $R_0$ ) and the kinetic properties of ligand-receptor complexes ( $k_{ec}$  and  $k_{off}$ ). Interestingly, we find that the front speed has a maximum with respect to the intensity of forward binding reaction (a product of the forward rate constant of ligand-receptor binding and the number of cell surface receptors). In particular, for any given value of the kinetic rate constants, there exists an optimal number of cell surface receptors. The speed of the front is maximal at this optimal value; see Fig. 4 *B* for the typical one-dimensional cut through the two-parameter plot in Fig. 4 *A*.

The nonmonotonic dependence of the front speed on the number of surface receptors and/or the forward binding rate constant is a result of the particular nature of coupling in autocrine relays. A sufficient number of cell surface receptors must be occupied to sustain the protease activation; this explains the ascending part of the curve. At the same time, the traveling front is slowed down when ligand spends most of its time bound to cell surface receptors; this qualitatively explains the descending part of the curve. A more detailed study of the parametric dependences of the

velocity will be presented elsewhere. The maximum in the dependence of the front speed on  $k_{on}R_0$  is the robust property of autocrine relays; it exists for any value of the threshold in the nonlinearity and the rate constants of dissociation and internalization. The speed of the front depends on the kinetic properties of ligand-receptor binding. Hence, it is not possible to compare front speeds in ligand-receptor systems based only on the corresponding equilibrium binding constant.

The height of the medium can be easily adjusted in cell and tissue culture assays. Fig. 5 *A* presents the dependence of the front speed on the ratio of the geometric and dynamic length scales in the problem (i.e., ratio of  $h$  and  $L_x$ ). When the ratio of these two length scales is small, the front speed is an increasing function of the medium height. Once again, this is the result of the nature of coupling in autocrine epithelial layers. For small height of the medium, the time interval between successive binding events of secreted ligand is short; the ligand spends a large fraction of its time in the bound form. Consequently, increasing the height of the medium increases both the duration and the span of the ligand trajectories and, as a result, the speed of the propagating front. In this regime, the fronts are essentially one-dimensional, in a sense that they are nearly uniform in the vertical direction; see the two top profiles in Fig. 5 *B*. This is easy to understand: the small value of the medium height translates into the low value of the Damköhler number,  $\alpha$ , that determines variation of the solution in the vertical direction; see Eqs. 8–12. In fact, a conventional “thin fin” approximation (Deen 1998) derived in the limit  $\alpha \rightarrow 0$  captures these fronts and their dependence on the height of the medium very accurately (results not shown).

When the height of the medium is comparable to the dynamical length scale  $L_x$  of the problem, the fronts become fully two-dimensional; see the two bottom profiles in Fig. 5 *B*. The dependence of the front speed on the medium's height  $h$  asymptotically approaches a constant value, Fig. 5 *A*. This behavior can be explained in terms of the results of a recent analysis of autocrine loops in the semi-infinite medium (Shvartsman et al., 2001). The statistical properties of both the vertical and the lateral spans of the random trajectories followed by autocrine ligands are characterized by the single length scale given by  $L_x$ . Specifically, half of the ligand trajectories are captured for the first time before their maximal lateral displacement reaches  $L_x$ . This is precisely the dynamical length scale in our problem; see Eq. 6. In other words, autocrine loops are spatially localized even in the semiinfinite medium. This means that, above some critical value, increasing the height of the medium would stop contributing to the effective range of the messenger variable in our problem. Consequently, the dependence of the front speed on the height of the medium should vanish at high ratios of the geometric and the dynamic length scales in the problem, Fig. 5 *A*.

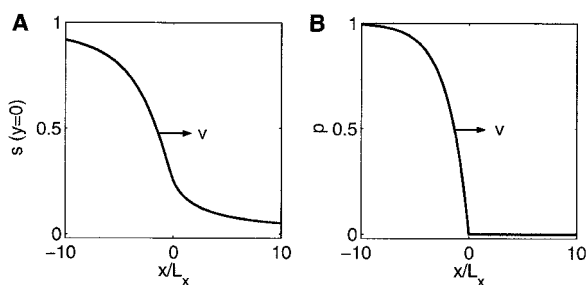


FIGURE 3 A traveling front in the ligand-limited regime with fast binding and sharp nonlinearity of protease activation (see Appendix A). (A) and (B) present the profiles of the extracellular ligand and ligand-releasing protease, respectively. The arrows denote the direction of wave's motion. The value of the dimensionless velocity is  $v = 1.967$ ; the threshold in the Heaviside function,  $c_0 = 0.25$ . Other dimensionless model parameters are  $\alpha = 55.36$ ,  $\beta = 0.5$ ,  $\tau_s = 5.439 \times 10^{-4}$  (based on  $k_{on} = 1 \times 10^2 \mu\text{M}^{-1} \text{ min}^{-1}$ ,  $R_0$  is based on  $5 \times 10^4$  receptors/cell surface area ( $25 \mu\text{m}^2$ ),  $k_{ec} = 0.1 \text{ min}^{-1}$ ,  $k_{off} = 0.1 \text{ min}^{-1}$ ,  $D = 1 \times 10^{-10} \text{ m}^2 \text{ s}^{-1}$ ,  $k_p = 0.01 \text{ min}^{-1}$ ,  $h = 1 \times 10^3 \mu\text{m}$ ).

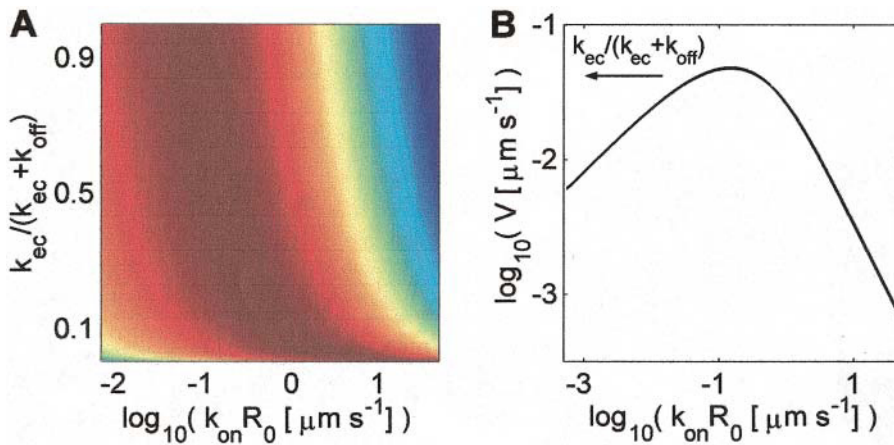


FIGURE 4 Dependence of the dimensional front speed on the kinetic and transport parameters in the ligand-limited regime with fast binding and sharp nonlinearity of protease activation (see Appendix A). (A) Dependence on the rate of forward binding on the forward-binding rate constant,  $k_{on}R_0$ , ligand-induced internalization rate constant  $k_{ec}$  and complex dissociation constant  $k_{off}$ . The dark red area corresponds to the maximal value of the velocity ( $v \approx 4 \times 10^{-2} \mu\text{m s}^{-1}$ ). Conversely, the dark blue area denotes the minimal value of the velocity ( $V \approx 4 \times 10^{-4} \mu\text{m s}^{-1}$ ). The threshold in the Heaviside function  $c_0 = 0.25$ . Other model parameters are  $h = 1 \times 10^3 \mu\text{m}$ ,  $D = 1 \times 10^{-10} \text{m}^2 \text{s}^{-1}$ ,  $k_p = 0.01 \text{min}^{-1}$ . (B) A one-dimensional cut ( $k_{ec}/(k_{ec} + k_{off}) = 0.5$ ) through the two-parameter plot in (A). The arrows indicate that increasing the ratio  $k_{ec}/(k_{ec} + k_{off})$  shifts the velocity maximum to a lower value of  $k_{on}R_0$ .

### Numerical simulations of propagating fronts

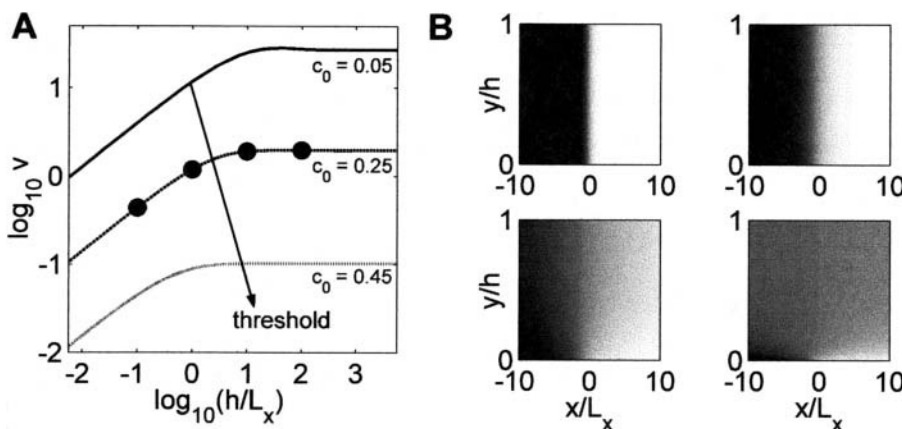
To test the predictions of the asymptotic analysis, we carried out numerical simulations of the full model described by Eqs. 8–12. The spatial derivatives in Eqs. 8 and 12 were replaced by finite differences and the resulting set of ODEs was solved using an efficient explicit solver for parabolic partial differential equations (Sommeijer et al., 1998).

Our main result can be summarized as follows: traveling fronts predicted in the simplified model exist for a wide range of parameters in the full model. Moreover, they exhibit the properties predicted by the analysis of the simplified model.

Fig. 6, A and B presents the profile of the fully developed front computed in the full model with the Hill nonlinearity, a nonzero value of the time scale of ligand-receptor complex, and a nonnegligible ratio of the ligand and receptor generation rates. This front was computed in a transient

simulation that started with the system in the “off state” and followed the evolution of a localized disturbance activating the ligand release. After the initial transient, this disturbance evolves into a fully developed self-similar solution—a constant speed front, Fig. 6 C. Fig. 6 D shows that, in agreement with the predictions of the analysis of the ligand-limited regime with fast binding and sharp nonlinearity of protease activation, the speed of the fronts in the full model exhibits a maximum with respect to the intensity of the binding process ( $k_{on}R_0$ ).

We used numerical simulations of the full model to analyze the interaction of propagating fronts with heterogeneities in the cellular layer. Our computational experiments are motivated by recent observations of Mandell and co-workers (Mandell et al., 2001). They have visualized the spatiotemporal dynamics of ERK2/MAPK activation that were induced in the layer of astroglial cells by a localized injury. Such a stimulus induced a wave-like transient that



(25  $\mu\text{m}^2$ ),  $k_{ec} = 0.1 \text{min}^{-1}$ ,  $k_{off} = 0.1 \text{min}^{-1}$ ,  $D = 1 \times 10^{-10} \text{m}^2 \text{s}^{-1}$ ,  $k_p = 0.01 \text{min}^{-1}$ ). (B) Color maps of the distributions  $s(\zeta, \eta)$  of the ligand in a traveling wave in both horizontal and vertical directions, with  $c_0 = 0.25$ . The spatial distributions of the ligand correspond to the filled circles in (A). The profiles were computed for  $\log_{10}(h/L_x) = -1, 0, 1$ , and  $2$ . The dark/bright regions correspond to the on/off steady states ( $s = 1, s = 0$ ), respectively.

FIGURE 5 Dependence of the wave propagation velocity on the ratio of the geometric length scale  $h$  and the dynamic length scale  $L_x$  in the ligand-limited regime with fast binding and sharp nonlinearity of protease activation (see Appendix A). The relationship between the dimensional ( $V$ ) and the dimensionless ( $v$ ) velocity is given by  $V = vL_xk_p$ . (A) Dependence of the dimensionless velocity on the ratio  $h/L_x$  computed for several thresholds  $c_0$  in the Heaviside function. The propagation velocity increases with the ratio until  $\log_{10}(h/L_x) \gg 1$ . Above this value, the velocity does not depend on this geometric parameter. The parameters are  $\beta = 0.5$ ,  $\tau_s = 5.439 \times 10^{-4}$  (based on  $k_{on} = 1 \times 10^2 \mu\text{M}^{-1} \text{min}^{-1}$ ,  $R_0$  is based on  $5 \times 10^4$  receptors/cell surface area

propagated away from the injured region of the epithelium, Fig. 3 in Mandell et al. (2001). They have suggested that this effect is mediated by a paracrine relay mechanism that is initiated at the place of injury. To support their hypothesis, they have shown that waves induced by the localized mechanical stimulus can “jump over” the gaps in the cellular layer. Hence, signal transmission is not mediated by direct cell-cell contact, but depends on diffusing signal.

Fig. 7 illustrates that traveling waves in the model of autocrine relays can “jump” over the heterogeneities in the cellular layer. This behavior is not unexpected, inasmuch as the mechanism of signal transmission is mediated by diffusion through the extracellular medium. What is interesting, however, is that the fronts can be both accelerated and impeded by the heterogeneities. This effect can be explained by the maximum in the dependence of the front speed on the number of cell surface receptors, Fig. 6 D. When the parameters of the monolayer correspond to the ascending part of the curve, the front is slowed down by the heterogeneity. In this regime, the heterogeneity provides a localized break in the positive feedback loop, Fig. 7 B. However, to the right of the maximum, when the front speed is a decreasing function of the number of receptors, the front will be accelerated by the local heterogeneity. In this regime, the front motion in the unperturbed layer is slowed down by frequent ligand-receptor binding. Thus, heterogeneity characterized by the absence of cell surface receptors provides a localized “escape path” for autocrine ligands, increasing

the range of their action, Fig. 7 D. Notice that in both cases the fronts regain the constant velocity after their interaction with local heterogeneity. We have found that for the front to “jump across the bump,” the size of heterogeneity has to be of the order of the dynamic length scale in the problem,  $L_x = (Dk_{er})/k_{on}Q_r$ , Fig. 7 C. These computational experiments underscore the unusual properties of traveling waves in autocrine systems. We can also predict the effect of other heterogeneities, e.g., in the value of ligand diffusivity. For example, in the regime when ligand binding slows down the front (the descending part of the curve in Fig. 4 B), a “defect” with increased diffusivity will speed up the front.

Our main results were obtained in the limit of sharp nonlinearity in protease activation (large Hill coefficient in sigmoidal function). Throughout this study, we have also assumed that there is no time delay in coupling between the level of occupied receptors and the rate of protease activation. We analyzed the limitations/applicability of both of these approximations. Our findings can be summarized as follows. First, the asymptotic results provide a very reasonable approximation for the velocity even for a much lower level of cooperativity. In fact, the true velocity for Hill coefficient,  $n = 2$ , differs from the asymptotic value by just 25%. This robustness is quite remarkable; see Fig. 8 A. In addition, we have used numerical methods for PDEs with time delays (Guglielmi et al., 2001) and continuation techniques for the heteroclinic orbits in problems with delays (Engelborghs et al., 2001), to examine the effect of

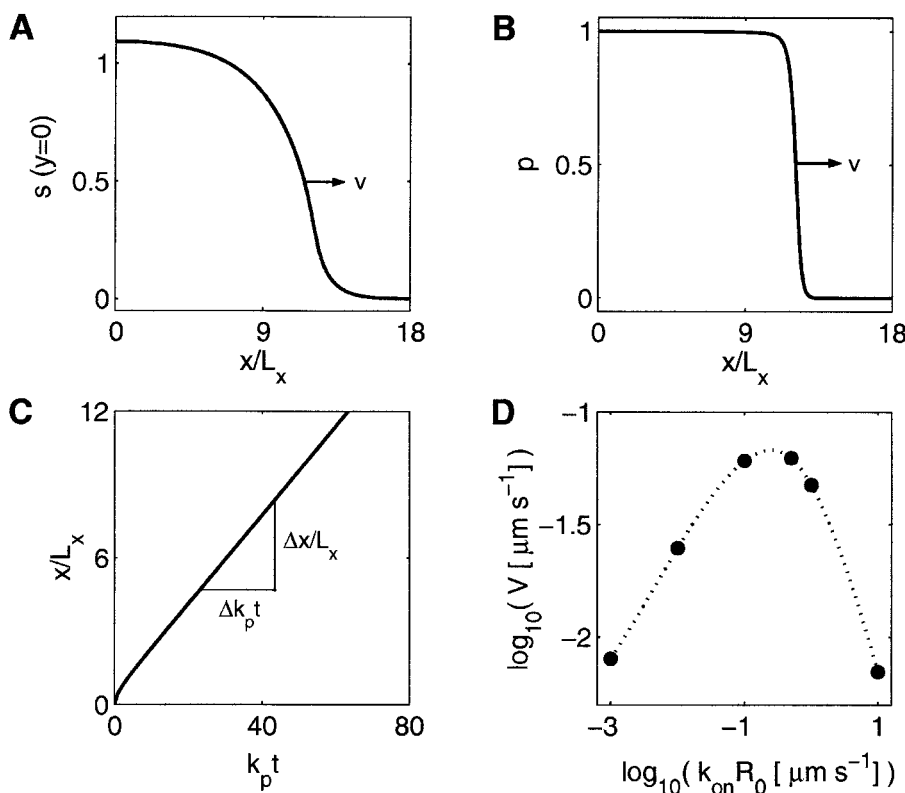
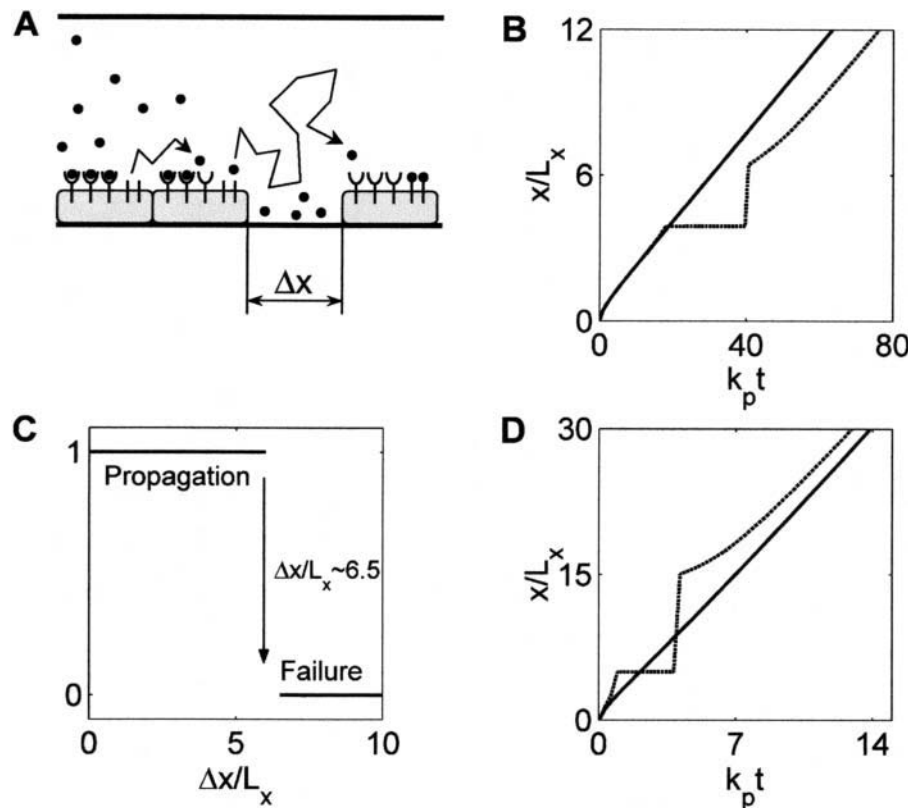


FIGURE 6 Numerical analysis of the full model. (A) and (B) Ligand and protease distributions computed across the front. The ligand release function is modeled by a Hill function  $\sigma(c) = c^n/(k^n + c^n)$ , with  $k = 0.25$  and  $n = 5$ . Other parameters are  $\alpha = 1$ ,  $\beta = 0.5$ ,  $\gamma = 0.2$ ,  $\tau_c = 0.1$ ,  $\tau_s = 3.334$ , and  $\tau_r = 2$  (based on  $k_{on} = 1.807 \mu\text{M}^{-1} \text{min}^{-1}$ ,  $R_0 = Q_r/k_{er}$  is based on  $5 \times 10^4$  receptors/cell surface area ( $Q_r = 500$  receptors/cell surface/min,  $k_{er} = 0.01 \text{ min}^{-1}$ , cell surface area  $25 \mu\text{m}^2$ ),  $k_{ec} = 0.1 \text{ min}^{-1}$ ,  $k_{off} = 0.1 \text{ min}^{-1}$ ,  $D = 1 \times 10^{-10} \text{ m}^2 \text{ s}^{-1}$ ,  $k_p = 0.02 \text{ min}^{-1}$ ,  $h = 1 \times 10^3 \mu\text{m}$ ,  $Q_l = g_{tg_p}/k_p = 50$  ligand molecules/cell surface/min). (C) The wave velocity was computed from the linear part of the dependence of the front position on time. (D) Dependence of the wave propagation velocity on the ligand-receptor affinity  $k_{on}R_0$ . The points are the results of the numerical analysis; the curve is drawn to guide the eye. The values of the parameters of the Hill nonlinearity and the other dimensional model parameters (except  $k_{on}$  and  $R_0$ ) are the same as in (A) and (B).



**FIGURE 7** Interaction of fronts with heterogeneities in the cellular layer. (A) The heterogeneities can both accelerate and slow down the fronts. The parameter  $\Delta x$  shows an extent of the heterogeneity. (B and D) The location of the front as a function of time in an intact (solid line) and damaged layer (broken line). (B) The case of low binding rate,  $k_{on}R_0 = 0.1 \mu\text{ms}^{-1}$  (based on  $k_{on} = 1.807 \mu\text{M}^{-1}\text{min}^{-1}$ ). The extent of the damaged tissue is  $\Delta x/L_x = 2.5$ . The values of the parameters of the Hill nonlinearity and the other model parameters are the same as in Fig. 6, A and B. (C) An increase of the heterogeneity extent stops the traveling front. It happens for  $\Delta x/L_x \sim 6.5$  in the case of the low binding rate; see (B). (D) The case of high ligand-receptor affinity  $k_{on}R_0 = 10 \mu\text{ms}^{-1}$  (based on  $k_{on} = 1.807 \times 10^2 \mu\text{M}^{-1}\text{min}^{-1}$ ). The extent of the damaged tissue is  $\Delta x/L_x = 10$ . Other parameters are as in Fig. 6, A and B.

delays on the fronts in our model. The argument of the sigmoidal function depended on the level of occupancy at a previous moment in time:  $\sigma(c(t - t_D))$ . We have found that the existence of fronts is preserved in the presence of delays and that the front speed smoothly depends on the magnitude of time delay. Hence, the fronts are robust with the respect to time delays in between receptor occupancy and protease activation. The general effect of delays is to reduce the front speed, Fig. 8 B. As there are more experimental results on long-range cell communication in autocrine and paracrine relays, additional biophysical effects such as nonspecific binding and ligand recycling can be included in the models.

The  $\tau_c \ll 1$  assumption can be readily relaxed. Fig. 8 C presents the dependence of the front speed on this parameter. The general effect of increasing the time scale for ligand dynamics is to slow the front speed down.

## CONCLUSIONS

We have developed a mechanistic model of autocrine relays. The model enables a systematic analysis of nonlinear interaction between ligand release, transport, and binding. Our transport model accounts for the nonlocal coupling between different regions of the epithelial layer; the range of the coupling is directly related to the transport, binding, and endocytosis of the secreted ligand. When combined with a positive feedback by ligand release, the model robustly

predicts the existence of propagating fronts. These fronts travel at constant speeds and can deliver signals to arbitrary distances. This wave-like propagation is very different from the one that relies on pure diffusion. Specifically, we predict the existence of traveling waves mediated by the autocrine release of growth factors. In other systems, traveling waves can be mediated by the regulated release of extracellular calcium, ATP, and cAMP (Kessler and Levine, 1993; Tang and Othmer, 1995; Tang et al., 1996; Palsen et al., 1997; D'andrea et al., 1998; Muller et al., 1998; Sneyd et al., 1998; Homolya et al., 2000; Scemes et al., 2000; Dormann et al., 2001; Shiga et al., 2001; Hofer et al., 2002; Schuster et al., 2002). The fronts mediated by autocrine loops have a number of unusual properties, such as a nonmonotonic dependence of the front speed on the total number of surface receptors and/or the forward binding rate constant. Wave-like patterns of intercellular communication can rely on multiple mechanisms. In several systems, a combination of paracrine and gap-junctional communication has been described (Hirata et al., 1998; Sauer et al., 2002). The physiological significance of these waves can range from robust and long-range signal delivery in normal tissue physiology (e.g., in response to injury; Mandell et al., 2001; Katz et al., 2002) to wave-mediated patterning of epithelial tissues (a propagating wave can leave a patterned state behind).

The predicted velocities of fronts in paracrine relays are dictated by the time scale of protease activation and by the



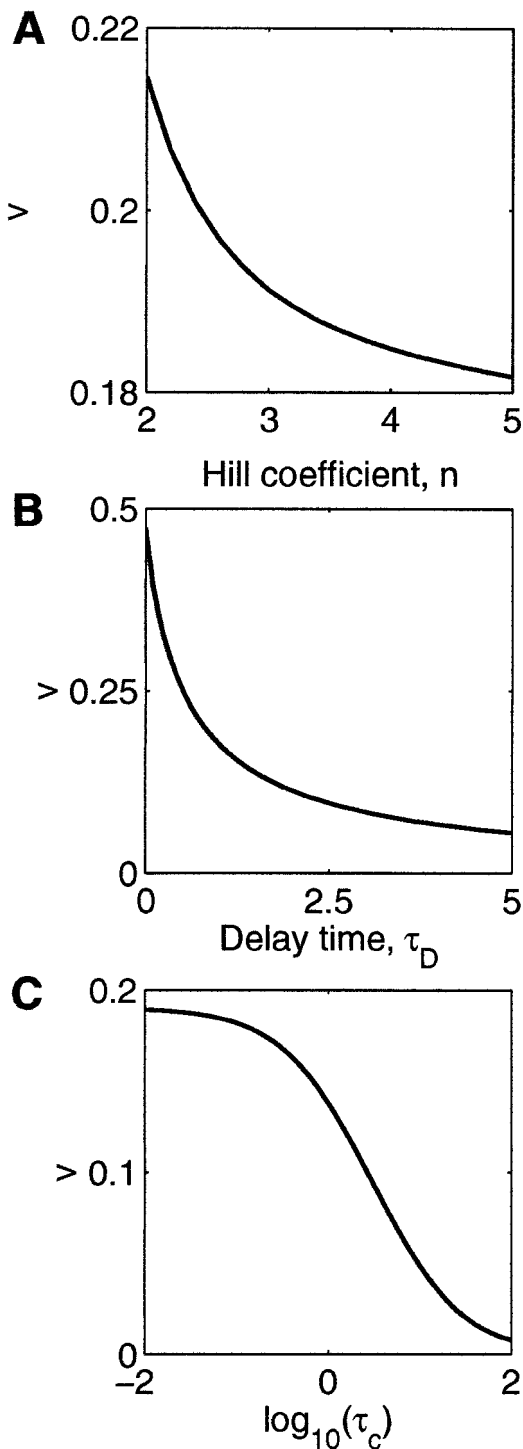


**FIGURE 8** Robustness of traveling fronts with respect to several modifications in the model. The relationship between the dimensional ( $V$ ) and the dimensionless ( $v$ ) velocity is given by  $V = vL_x k_p$ . (A) Dimensionless velocity monotonically decreases with growing value of the Hill coefficient  $n$  in the sigmoidal nonlinearity. For  $n = 2$ , the difference between dimensionless velocity of the full model and the velocity of the simplified model with sharp nonlinearity of protease activation in the ligand-limited regime ( $n \rightarrow +\infty$ ,  $\tau_c \rightarrow 0$ ,  $\gamma \rightarrow 0$ ) is  $\sim 25\%$ . For  $n = 5$ , the difference is only  $\sim 4\%$ . (B) Velocity of wave propagation monotonically decreases with increasing time delay in the sigmoidal nonlinearity of protease activation.

effective diffusivity determined by the combination of the ligand diffusion coefficient and the cell surface receptor density. The velocity of waves in autocrine relays mediated by secreted growth factors is lower than the velocity observed in axonal propagation and in the intracellular waves. On the other hand, these waves might operate in the processes of developmental pattern formation (Freeman, 2000; Freeman and Gurdon, 2002) and tissue remodeling in response to injury. At this point, one has to be careful in comparing our predictions to the observations of fronts in paracrine relays in growth factor systems. The reported experiments were done in large dishes, where medium convection could contribute to the increase of the apparent propagation velocity (Mandell et al., 2001; Katz et al., 2002).

We have considered only planar fronts. Our preliminary results indicate that convex/concave fronts will move slower/faster than the planar fronts for the same values of kinetic/transport parameters. This is expected from the behavior of conventional trigger waves in reaction-diffusion systems (Mikhailov, 1994). Hence, we expect the planar interfaces to be stable with respect to the lateral perturbations. In the future, it will be interesting to determine if autocrine relays can support fully two-dimensional fronts, such as the cusp-like interfaces described in (Brazhnik and Tyson, 1999). Recent experiments on paracrine waves in truly three-dimensional geometries, such as tumor spheroids, make the multidimensional extension of our analysis particularly relevant (Sauer et al., 2002).

At this point, there is no direct evidence for traveling waves mediated by the regulated secretion of peptide growth factors. Recently, however, a paracrine mechanism has been proposed to cause the wave-like spread of signaling activity induced by localized mechanical stimulus (Mandell et al., 2001). In addition, long-range cell communication mediated by the interaction between paracrine growth factors and ERK2 signaling has been observed in cell culture experiments with wounded osteoblast monolayers (Katz et al., 2002). There, fibroblast growth factors have been proposed as paracrine signals. A wealth of experiments supporting the release-mediated positive feedback in growth factor systems indicates that these waves can be observed (Hunter, 1998; Carpenter, 1999; Dent et al., 1999; Fan and Derynck, 1999; Gechtman et al., 1999; Moghal and Sternberg, 1999; Albanell et al., 2001; Chen et al., 2001; Gschwind et al., 2001; Ma et al., 2001; Merlos-Suarez et al., 2001; Murphy et al., 2001; Carraway and Sweeney, 2002; Diaz-Rodriguez

Dimensionless time delay  $\tau_D$  is plotted with units  $1/k_p$  (when  $k_p = 0.01 \text{ min}^{-1}$ ). The figure means that the wave propagation will not stop for the time delay 500 min and less. (C) Increase of the relative time scale of ligand-receptor complex processes  $\tau_c$  slows down the front. The other dimensionless model parameters and parameters of Hill nonlinearity in the studies (A) and (C) were kept at the same values as in Fig. 6, A and B; in the study, (B) used the same values as in Fig. 5 A, and  $\alpha = 0.1$ .

et al., 2002; Montero et al., 2002). Usually, this feedback is studied in cell culture, where cells are randomly dispersed on the surface. We predict that experiments with confluent cell monolayers or with model epithelial layers will uncover traveling waves mediated by autocrine growth factors. The EGFR network is a particularly promising experimental system. The experiments require an ability to locally stimulate ligand release and to follow the progress of activation across the cellular layer. Localized stimulation can be mechanical, chemical, or rely on gamma or UV radiation. Excitation can be followed either *in situ* (e.g., using fluorescent reporters) or *ex situ* (e.g., using Western blot epithelial layers at different time points). The A431 carcinoma cell line with a positive EGFR/MAPK/TGF $\alpha$  feedback is a good experimental system for these studies (Dent et al., 1999; Shvartsman et al., 2002).

Almost invariably, nonlinear traveling waves in cell communication are modeled as reaction-diffusion systems, where the amplification processes in the active medium happen in the same region as transport. In our model, these processes are separated in a sense that active processes at different parts of the surface are nonlocally coupled by diffusion through the volume. The properties of traveling waves in such systems are yet to be characterized in details. From the mathematical standpoint, nonlinear waves in multiphase reaction-transport systems were studied by Othmer (1975).

Traveling waves in autocrine and paracrine relays can propagate through the discontinuities in the phase that generates the active signal. *In vitro*, this property can be revealed by experiments with “scratched” monolayers, as was done in an elegant study by Mandell (et al., 2001). *In vivo*, this setup can be realized by generating the clones of cells lacking the receptor for the paracrine ligand; see Tabata (2001) for the recent review of relevant genetic techniques. In both cases, experiments should be spatially resolving and cannot rely just on localized measurements.

The positive feedback from ligand binding to ligand release is just one of the many regulatory patterns in autocrine and paracrine networks. Some of the other mechanisms involve binding-stimulated receptor shedding (Ni et al., 2001), decrease of receptor mRNA stability (Sturtevant et al., 1994), and release of extracellular ligand/binding components (Guan et al., 2001; Freeman and Gurdon, 2002; Gerlitz and Basler, 2002). The physiological significance of these processes is only starting to be appreciated.

The next stage of modeling should account for the dynamics of intracellular signaling. A number of “lumped” models of EGFR signaling can be incorporated into our models of autocrine epithelial layers (Bhalla and Iyengar, 1999; Kholodenko et al., 1999; Brightman and Fell, 2000; Haugh et al., 2000; Schoeberl et al., 2002). For this, a model of protease dynamics is necessary. A simplified description, accounting for the stimulation-induced downregulation of the protease and the kinetic patterns of EGFR ligand release,

has been recently developed (Dong and Wiley, 1999; Fan and Derynck, 1999; Gechtman et al., 1999; Doedens and Black, 2000; Shvartsman et al., 2002). A growing number of studies of regulated ligand release can be used to develop and validate a more detailed model. This model would simultaneously account for multiple species and processes leading to binding-induced ligand release (Albanell et al., 2001; Merlos-Suarez et al., 2001; Umata et al., 2001; Zhang et al., 2001; Diaz-Rodriguez et al., 2002; Kheradmand and Werb, 2002; Montero et al., 2002; Sunnarborg et al., 2002).

We have emphasized the positive feedback and activation processes in autocrine relays. This is sufficient to capture the leading part of the propagating wave. Various intracellular processes, working on the time scales of minutes to hours, may switch the system off. This would convert the traveling front to a traveling pulse. When the deactivation processes are slow, the traveling pulse has a well-defined front edge (Meron, 1992), and pulse speed is well-approximated by the analysis that neglects deactivation in the back of the wave. Increasing the ratio of the time scales of deactivation and activation will eventually destroy the traveling pulse. In the case of conventional reaction-diffusion systems, this transition is through the saddle-node bifurcation (Mikhailov, 1994). Among the processes that contribute to the deactivation in autocrine relays are well-established adaptation in growth-factor-induced ERK2 signaling, downregulation of level of ligand precursor, and downregulation of the protease activity. The last process has been clearly demonstrated in the recent experiment of Doedens and Black (2000). The TACE protease that regulates the availability of EGFR ligands (Sunnarborg et al., 2002) is activated by a number of intracellular pathways. The activated form of this enzyme then cleaves the ectodomains of transmembrane molecules. At the same time, the active form of the enzyme is primed for degradation and is cleared from the surface through the endocytic pathway.

## APPENDIX

The analytical solution is constructed in the limiting case of  $\tau_c \rightarrow 0$ ,  $\gamma \rightarrow 0$ , and  $\sigma(c) = H(c - c_0)$ , where  $H(x)$  is the Heaviside function and  $c_0$  is the threshold. Under these assumptions, we have  $r = 1$  and  $c(\xi, \tau) = \bar{s}(\xi, \tau)$  on the time scale of the wave, so Eqs. 9–12 simplify to

$$\frac{\partial p}{\partial \tau} = -p + H(\bar{s} - c_0), \quad (\text{A1})$$

$$\left( \frac{\partial s}{\partial \eta} - \alpha \beta s \right) \Big|_{\eta=0} = -\alpha \beta p \quad \frac{\partial s}{\partial \eta} \Big|_{\eta=1} = 0. \quad (\text{A2})$$

We are looking for the traveling wave solutions  $s = s(\zeta - v\tau, \eta)$ ,  $p = p(\zeta - v\tau)$  connecting the steady state  $s = 1$ ,  $p = 1$  at  $\zeta = -\infty$  with the steady state  $s = 0$ ,  $p = 0$  at  $\zeta = +\infty$ , moving with speed  $v > 0$  to the right. Introducing the reference frame moving with the wave

$$\xi \equiv \zeta - v\tau, \quad (\text{A3})$$

and rewriting Eqs. 8 and A1 in terms of  $\xi$ , we obtain

$$\frac{\partial^2 s}{\partial \xi^2} + \mathbf{v} \tau_s \frac{\partial s}{\partial \xi} + \frac{1}{\alpha^2} \frac{\partial^2 s}{\partial \eta^2} = 0, \quad (\text{A4})$$

$$\mathbf{v} \frac{\partial p}{\partial \xi} - p + H(-\xi) = 0, \quad s(0, 0) = c_0, \quad (\text{A5})$$

where we assumed that  $s(\xi, 0)$  is a monotonically decreasing function of  $\xi$  and placed the point of the onset of the protease production at the origin.

Eq. A5 can be straightforwardly integrated:

$$p(\xi) = H(-\xi)(1 - \exp(\xi/\mathbf{v})). \quad (\text{A6})$$

This solution can be substituted into Eqs. A2 and A4, which can then be solved by separation of variables. Let us look for the solution of Eqs. A2 and A4 in the form

$$s(\xi, \eta) = p(\xi) + \sum_{n=1}^{\infty} \phi_n(\xi) \psi_n(\eta), \quad (\text{A7})$$

where  $\psi_n(\eta)$  are the orthonormal eigenfunctions of the Sturm-Liouville problem

$$\psi_n'' + \lambda_n^2 \psi_n = 0, \quad \psi_n'(0) - \alpha \beta \psi_n(0) = 0, \quad \psi_n'(1) = 0. \quad (\text{A8})$$

---


$$\phi_n^+(\xi) = \frac{\alpha \sin \lambda_n \exp\{-[\mathbf{v} \alpha \tau_s + (4\lambda_n^2 + \mathbf{v}^2 \alpha^2 \tau_s^2)^{1/2}] \xi / (2\alpha)\}}{[2\lambda_n(\lambda_n + \sin \lambda_n \cos \lambda_n)]^{1/2}} \times \frac{\mathbf{v}[\tau_s \alpha^2(\tau_s \mathbf{v}^2 + 1) + 2\lambda_n^2] - \alpha(\tau_s \mathbf{v}^2 + 1)(4\lambda_n^2 + \mathbf{v}^2 \alpha^2 \tau_s^2)^{1/2}}{[\mathbf{v}^2 \lambda_n^2 - \alpha^2(\tau_s \mathbf{v}^2 + 1)](4\lambda_n^2 + \mathbf{v}^2 \alpha^2 \tau_s^2)^{1/2}}, \quad (\text{A16})$$


---

$s(-\infty, 0) = 1$ . We should also use the fact that  $s$  together with its first derivatives must be continuous at  $\xi = 0$ . In view of Eq. A7, this translates to

$$\sum_{n=1}^{\infty} \phi_n^+(0) \psi_n(\eta) = \sum_{n=1}^{\infty} \phi_n^-(0) \psi_n(\eta), \quad (\text{A12})$$

$$\sum_{n=1}^{\infty} \psi_n(\eta) \frac{d\phi_n^+}{d\xi} \Big|_{\xi=0} = \sum_{n=1}^{\infty} \psi_n(\eta) \frac{d\phi_n^-}{d\xi} \Big|_{\xi=0} - \mathbf{v}^{-1} \quad (\text{A13})$$

Once again, multiplying Eqs. A12 and A13 by  $\psi_n$ , integrating over  $\eta$ , and combining them with the behavior at infinity, we obtain that  $\phi_n^{\pm}$ , which should satisfy the following boundary equation,

$$\phi_n^{\pm}(\pm\infty) = 0, \quad \phi_n^+(0) = \phi_n^-(0) \quad (\text{A14})$$

$$\frac{d\phi_n^+}{d\xi} \Big|_{\xi=0} = \frac{d\phi_n^-}{d\xi} \Big|_{\xi=0} - \left[ \frac{2}{\lambda_n(\lambda_n + \sin \lambda_n \cos \lambda_n)} \right]^{1/2} \frac{\sin \lambda_n}{\mathbf{v}} \quad (\text{A15})$$

After a rather long, but straightforward calculation, we obtain

and

---


$$\phi_n^-(\xi) = \frac{\alpha \sin \lambda_n \exp\{-[\mathbf{v} \alpha \tau_s - (4\lambda_n^2 + \mathbf{v}^2 \alpha^2 \tau_s^2)^{1/2}] \xi / (2\alpha)\}}{[2\lambda_n(\lambda_n + \sin \lambda_n \cos \lambda_n)]^{1/2}} \times \frac{\mathbf{v}[\tau_s \alpha^2(\tau_s \mathbf{v}^2 + 1) + 2\lambda_n^2] + \alpha(\tau_s \mathbf{v}^2 + 1)(4\lambda_n^2 + \mathbf{v}^2 \alpha^2 \tau_s^2)^{1/2}}{[\mathbf{v}^2 \lambda_n^2 - \alpha^2(\tau_s \mathbf{v}^2 + 1)](4\lambda_n^2 + \mathbf{v}^2 \alpha^2 \tau_s^2)^{1/2}} - \frac{2\alpha^2(\tau_s \mathbf{v}^2 + 1) \sin \lambda_n \exp(\xi/\mathbf{v})}{[\mathbf{v}^2 \lambda_n^2 - \alpha^2(\tau_s \mathbf{v}^2 + 1)][2\lambda_n(\lambda_n + \sin \lambda_n \cos \lambda_n)]^{1/2}}. \quad (\text{A17})$$


---

A simple calculation gives

$$\lambda_n \tan(\lambda_n) = \alpha \beta \quad n = 1, 2, 3, \dots, +\infty \quad (\text{A9})$$

Substituting this solution into Eq. A7 and using it in the self-consistency condition in Eq. A5, we obtain the implicit expression for the speed of the traveling wave,

---


$$c_0 = \sum_{n=1}^{\infty} \frac{4\alpha \lambda_n^2 \sin \lambda_n \cos \lambda_n / (\lambda_n + \sin \lambda_n \cos \lambda_n)}{\alpha(\tau_s \mathbf{v}^2 + 1)(4\lambda_n^2 + \mathbf{v}^2 \alpha^2 \tau_s^2) + \mathbf{v}[2\lambda_n^2 + \alpha^2 \tau_s(\tau_s \mathbf{v}^2 + 1)](4\lambda_n^2 + \mathbf{v}^2 \alpha^2 \tau_s^2)^{1/2}}. \quad (\text{A18})$$


---

$$\psi_n(\eta) = [2\lambda_n / (\lambda_n + \sin \lambda_n \cos \lambda_n)]^{1/2} \cos(\lambda_n - \lambda_n \eta). \quad (\text{A10})$$

Substituting Eq. A7 into A4, multiplying it by  $\psi_n$ , and then integrating over  $\eta$ , we obtain an equation for  $\phi_n^{\pm}(\xi)$ , where  $\phi_n^+(\xi)$  and  $\phi_n^-(\xi)$  are the solutions for  $\xi > 0$  and  $\xi < 0$ , respectively:

$$\frac{d^2 \phi_n^{\pm}}{d\xi^2} + \mathbf{v} \tau_s \frac{d\phi_n^{\pm}}{d\xi} - \frac{\lambda_n^2}{\alpha^2} \phi_n^{\pm} = \left[ \frac{2}{\lambda_n(\lambda_n + \sin \lambda_n \cos \lambda_n)} \right]^{1/2} \frac{(1 + \mathbf{v}^2 \tau_s) \sin \lambda_n \exp(\xi/\mathbf{v}) H(-\xi)}{\mathbf{v}^2} \quad (\text{A11})$$


---

This equation has to be supplemented by the boundary conditions at  $\xi = 0$  and  $\xi \rightarrow \pm\infty$ . At infinity we must use the exact fact that  $s(+\infty, 0) = 0$  and

We thank Giovanni Samaey for help with the DDE-BIFTOOL software and Jim Mandell for many helpful discussions.

Our work has been supported by the National Science Foundation.

## REFERENCES

- Albanell, J., J. Codony-Servat, F. Rojo, J. M. Del Campo, S. Sauleda, J. Anido, G. Raspall, J. Giralit, J. Rosello, R. I. Nicholson, J. Mendelsohn, and J. Baselga. 2001. Activated extracellular signal-regulated kinases: association with epidermal growth factor receptor/ transforming growth factor  $\alpha$  expression in head and neck squamous carcinoma and inhibition by anti-epidermal growth factor treatments. *Cancer Res.* 61:6500–6510.
- Bang, A. G., and C. Kintner. 2000. Rhomboid and Star facilitate presentation and processing of the *Drosophila* TGF- $\alpha$  homolog Spitz. *Genes Dev.* 14:177–186.
- Bhalla, U., and R. Iyengar. 1999. Emergent properties of networks of biological signaling pathways. *Science.* 283:381–387.
- Brazhnik, P. K., and J. J. Tyson. 1999. Travelling waves and static structures in a two-dimensional exactly solvable reaction-diffusion system. *J. Phys. A. Math. G. E. N.* 32:8033–8044.
- Brightman, F. A., and D. A. Fell. 2000. Differential feedback regulation of the MAPK cascade underlies the quantitative differences in EGF and NGF signaling in PC12 cells. *FEBS Lett.* 482:169–174.
- Burke, P., K. Schooler, and H. S. Wiley. 2001. Regulation of epidermal growth factor receptor signaling by endocytosis and intracellular trafficking. *Mol. Cell. Biol.* 12:1897–1910.
- Carpenter, G. 1999. Employment of the epidermal growth factor receptor in growth factor-independent signaling pathways. *J. Cell Biol.* 146: 697–702.
- Carraway, K. L., and C. Sweeney. 2002. EGF receptor activation by heterologous mechanisms. *Cancer Cell.* 1:405–406.
- Casci, T., and M. Freeman. 1999. Control of EGF receptor signalling: lessons from fruitflies. *Cancer Met. Rev.* 18:181–201.
- Chen, N., W. Y. Ma, Q. B. She, E. Wu, G. Liu, A. M. Bode, and Z. Dong. 2001. Transactivation of the epidermal growth factor receptor is involved in 12-O-tetradecanoylphorbol-13-acetate-induced signal transduction. *J. Biol. Chem.* 276:46722–46728.
- D'andrea, P., A. Calabrese, and M. Grandolfo. 1998. Intercellular calcium signalling between chondrocytes and synovial cells in co-culture. *Biochem. J.* 329:681–687.
- Deen, W. M. 1998. Analysis of Transport Phenomena. Oxford University Press, New York.
- Dello, S., and E. Rovida. 2002. Transmodulation of cell surface regulatory molecules via ectodomain shedding. *Biol. Chem.* 383:69–83.
- Dent, P., D. Reardon, J. Park, G. Bowers, C. Logsdon, K. Valerie, and R. Schmidt-Ullrich. 1999. Radiation-induced release of transforming growth factor  $\alpha$  activates the epidermal growth factor receptor and mitogen-activated protein kinase pathway in carcinoma cells, leading to increased proliferation and protection from radiation-induced cell death. *Mol. Biol. Cell.* 10:2493–2506.
- DeWitt, A., J. Dong, H. Wiley, and D. Lauffenburger. 2001. Quantitative analysis of the EGF receptor autocrine system reveals cryptic regulation of cell response by ligand capture. *J. Cell Sci.* 114:2301–2313.
- Diaz-Rodriguez, E., J. C. Montero, A. Esparis-Ogando, L. Yuste, and A. Pandiella. 2002. Extracellular signal-regulated kinase phosphorylates tumor necrosis factor  $\alpha$ -converting enzyme at threonine 735: a potential role in regulated shedding. *Mol. Biol. Cell.* 13:2031–2044.
- Dobens, L. L., and L. A. Raftery. 2000. Integration of epithelial patterning and morphogenesis in *Drosophila* oogenesis. *Dev. Dyn.* 218:80–93.
- Doedens, J. R., and R. A. Black. 2000. Stimulation-induced down-regulation of tumor necrosis factor- $\alpha$  converting enzyme. *J. Biol. Chem.* 275:14598–14607.
- Dong, J. Y., and H. S. Wiley. 1999. Trafficking and proteolytic release of epidermal growth factor receptor ligands are modulated by their membrane-anchoring domains. *J. Biol. Chem.* 275:557–564.
- Doraiswamy, V., J. Parrot, and M. Skinner. 2000. Expression and action of transforming growth factor  $\alpha$  in normal ovarian surface epithelium and ovarian cancer. *Biol. Reprod.* 63:789–796.
- Dormann, D., J. Kim, P. Devreotes, and C. Weijer. 2001. cAMP receptor affinity controls wave dynamics, geometry and morphogenesis in *Dictyostelium*. *J. Cell Sci.* 114:2513–2523.
- Engelborghs, K., T. Luzyanina, and G. Samaey. 2001. DDE\_BIFTOOL v. 2.00 User Manual: A Matlab Package for Bifurcation Analysis of Delay Differential Equations. Technical Report TW-330. Department of Computer Science, Leuven.
- Fall, C., E. Marland, E. Wagner, and J. J. Tyson, editors. 2002. Computational Cell Biology. Springer, New York.
- Fan, H. Z., and R. Derynck. 1999. Ectodomain shedding of TGF- $\alpha$  and other transmembrane proteins is induced by receptor tyrosine kinase activation and MAP kinase signaling cascades. *EMBO J.* 18:6962–6972.
- Ferrell, J., and W. Xiong. 2001. Bistability in cell signaling: how to make continuous processes discontinuous, and reversible processes irreversible. *Chaos.* 11:221–236.
- Freeman, M. 1997. Cell determination strategies in the *Drosophila* eye. *Development.* 124:261–270.
- Freeman, M. 2000. Feedback control of intercellular signalling in development. *Nature.* 408:6810.
- Freeman, M., and J. B. Gurdon. 2002. Regulatory principles of developmental signaling. *Annu. Rev. Cell Dev. Biol.* 18:515–539.
- Gechtman, Z., J. L. Alonso, G. Raab, D. E. Ingber, and M. Klagsbrun. 1999. The shedding of membrane-anchored heparin-binding epidermal-like growth factor is regulated by the *Raf*/mitogen-activated protein kinase cascade and by cell adhesion and spreading. *J. Biol. Chem.* 274:28828–28835.
- Gerlitz, O., and K. Basler. 2002. Wingful, an extracellular feedback inhibitor of Wingless. *Genes Dev.* 16:1055–1059.
- Gschwind, A., E. Zwick, N. Prenzel, M. Leserer, and A. Ullrich. 2001. Cell communication networks: epidermal growth factor receptor transactivation as the paradigm for interreceptor signal transmission. *Oncogene.* 20:1594–1600.
- Guan, R., Y. Zhang, J. Jiang, C. Baumann, R. Black, G. Baumann, and S. Frank. 2001. Phorbol ester- and growth-factor-induced growth hormone (GH) proteolysis and GH-binding protein shedding: relationship to GH receptor downregulation. *Endocrinology.* 142:1137–1147.
- Guglielmi, N., E. L'Aquila, and E. Hairer. 2001. Implementing Radau IIA methods for stiff delay differential equations. *Computing.* 67:1–12.
- Guichard, A., B. Biehs, M. A. Sturtevant, L. Wickline, J. Chacko, and K. Howard. 1999. rhomboid and Star interact synergistically to promote EGFR/MAPK signaling during *Drosophila* wing vein development. *Development.* 126:2663–2676.
- Gurdon, J. B., and P. Y. Bourillot. 2001. Morphogen gradient interpretation. *Nature.* 413:797–803.
- Hagan, M., L. Wang, J. R. Hanley, J. S. Park, and P. Dent. 2000. Ionizing radiation-induced mitogen-activated protein (MAP) kinase activation in DU145 prostate carcinoma cells: MAP kinase inhibition enhances radiation-induced cell killing and G(2)/M-Phase arrest. *Radiat. Res.* 153:371–383.
- Harari, M., and S. Huang. 2001. Radiation response modification following molecular inhibition of epidermal growth factor receptor signaling. *Semin. Radiat. Oncol.* 11:281–289.
- Haugh, J., A. Huang, H. Wiley, A. Wells, and D. Lauffenburger. 1999. Internalized epidermal growth factor receptors participate in the activation of p21(ras) in fibroblasts. *J. Biol. Chem.* 274:34350–34360.
- Haugh, J., A. Wells, and D. Lauffenburger. 2000. Mathematical modeling of epidermal growth factor receptor signaling through the phospholipase C pathway: mechanistic insights and predictions for molecular interventions. *Biotechnol. Bioeng.* 70:225–238.

- Hirata, K., M. H. Nathanson, and M. L. Sears. 1998. Novel paracrine signaling mechanism in the ocular ciliary epithelium. *Proc. Natl. Acad. Sci. USA*. 95:8381–8386.
- Hofer, T., L. Venance, and C. Giaume. 2002. Control and plasticity of intercellular calcium waves in astrocytes: a modeling approach. *Biophys. J.* 22:4850–4859.
- Homolya, L., T. H. Steinberg, and R. C. Boucher. 2000. Cell to cell communication in response to mechanical stress via bilateral release of ATP and UTP in polarized epithelia. *J. Cell Biol.* 150:1349–1360.
- Hsu, T., D. McRackan, T. S. Vincent, and H. Gert de Couet. 2001. *Drosophila* Pin1 prolyl isomerase Dodo is a MAP kinase signal responder during oogenesis. *Nat. Cell Biol.* 3:538–543.
- Hunter, T. 1998. The Croonian Lecture 1997. The phosphorylation of proteins on tyrosine: its role in cell growth and disease. *Philos. Trans. R. Soc. Lond. B Biol. Sci.* 353:583–605.
- Hunter, T. 2000. Signaling—2000 and beyond. *Cell*. 100:113–127.
- Jordan, J., E. Landau, and R. Iyengar. 2000. Signaling networks: the origins of cellular multitasking. *Cell*. 103:193–200.
- Katz, R. W., S. Y. Teng, S. Thomas, and R. Landesberg. 2002. Paracrine activation of extracellular signal-regulated kinase in a simple in vitro model of wounded osteoblasts. *Bone*. 31:288–295.
- Keener, J. 1998. *Mathematical Physiology*. Springer, New York.
- Kessler, D. A., and H. Levine. 1993. Pattern formation in *Dictyostelium* via the dynamics of cooperative biological entities. *Phys. Rev. E*. 48:4801–4804.
- Kheradmand, F., and Z. Werb. 2002. Shedding light on sheddases: role in growth and development. *Bioessays*. 24:8–12.
- Kholodenko, B. N., O. V. Demin, G. Moehren, and J. B. Hoek. 1999. Quantification of short term signaling by the epidermal growth factor receptor. *J. Biol. Chem.* 274:30169–30181.
- Lauffenburger, D. A., L. L. Chu, A. French, G. Oehrtman, C. Reddy, A. Wells, S. Niyogi, and H. S. Wiley. 1996. Engineering dynamics of growth factors and other therapeutic ligands. *Biotech. Bioeng.* 52:61–80.
- Lauffenburger, D. A., K. E. Forsten, B. Will, and H. S. Wiley. 1995. Molecular/cell engineering approach to autocrine ligand control of cell function. *Ann. Biomed. Eng.* 23:208–215.
- Lauffenburger, D. A., and J. J. Linderman. 1993. *Receptors: Models for Binding, Trafficking, and Signalling*. Oxford University Press, New York.
- Lee, J. R., S. Urban, C. F. Garvey, and M. Freeman. 2001. Regulated intracellular ligand transport and proteolysis regulate EGF receptor activation in *Drosophila*. *Cell*. 107:161–171.
- Ma, Z., D. Webb, M. Jo, and S. Gonias. 2001. Endogenously produced urokinase-type plasminogen activator is a major determinant of the basal level of activated ERK/MAP kinase and prevents apoptosis in MDA-MB-231 breast cancer cells. *J. Cell Sci.* 114:3387–3396.
- Mandell, J. W., N. C. Gocan, and S. R. Vandenberg. 2001. Mechanical trauma induces rapid astroglial activation of ERK/MAP kinase: evidence for a paracrine signal. *Glia*. 34:283–295.
- Mantrova, E., and T. Hsu. 1998. Down-regulation of transcription factor CF2 by *Drosophila* Ras/MAP kinase signaling in oogenesis: cytoplasmic retention and degradation. *Genes Dev.* 12:1166–1175.
- Merlos-Suarez, A., and J. Arribas. 1999. Mechanisms controlling the shedding of transmembrane molecules. *Biochem. Soc. Trans.* 27:243–246.
- Merlos-Suarez, A., S. Ruiz-Paz, J. Baselga, and J. Arribas. 2001. Metalloprotease-dependent protransforming growth factor- $\alpha$  ectodomain shedding in the absence of tumor necrosis factor- $\alpha$ -converting enzyme. *J. Biol. Chem.* 276:48510–48517.
- Meron, E. 1992. Pattern formation in excitable media. *Phys. Rep.* 218:1–66.
- Mikhailov, A. S. 1994. *Foundations of Synergetics*. Springer, Berlin and New York.
- Moghal, M., and P. W. Sternberg. 1999. Multiple positive and negative regulators of signaling by the EGF-receptor. *Curr. Opin. Cell Biol.* 11:190–196.
- Montero, J., L. Yuste, E. Diaz-Rodriguez, A. Espasis-Ogando, and A. Pandiella. 2000. Differential shedding of transmembrane neuregulin isoforms by tumor necrosis-factor- $\alpha$ -converting enzyme. *Mol. Cell. Neurosci.* 16:631–648.
- Montero, J. C., L. Yuste, E. Diaz-Rodriguez, A. Esparis-Ogando, and A. Pandiella. 2002. Mitogen-activated protein kinase-dependent and -independent routes control shedding of transmembrane growth factors through multiple secretases. *Biochem. J.* 363:211–221.
- Muller, S. C., T. Mair, and O. Steinbock. 1998. Traveling waves in yeast extract and in cultures of *Dictyostelium discoideum*. *Biophys. Chem.* 72:37–47.
- Murphy, L., M. Cluck, S. Lovas, F. Otvos, R. Murphy, A. Schally, J. Permert, J. Larsson, J. Knezetic, and T. Adrian. 2001. Pancreatic cancer cells require an EGF receptor-mediated autocrine pathway for proliferation under serum-free conditions. *Br. J. Cancer*. 84:926–935.
- Ni, C. Y., M. P. Murphy, T. E. Golde, and G. Carpenter. 2001.  $\gamma$ -Secretase cleavage and nuclear localization of ErbB-4 receptor tyrosine kinase. *Science*. 294:2179–2181.
- Ogunnaike, B. A., and W. Ray. 1994. *Process Dynamics, Modeling, and Control*. University Press, Oxford.
- Othmer, H. G. 1975. Nonlinear wave propagation in reacting systems. *J. Math. Biol.* 2:133–163.
- Palsson, E., K. J. Lee, R. E. Golstein, J. Franke, R. H. Kessin, and E. Cox. 1997. Selection for spiral waves in the social amoebae *Dictyostelium*. *Proc. Natl. Acad. Sci. USA*. 94:13719–13723.
- Rutledge, B., K. Zhang, E. Bier, Y. Jan, and N. Perrimon. 1992. The *Drosophila* spitz gene encodes a putative EGF-like growth factor involved in dorsal-ventral axis formation and neurogenesis. *Genes Dev.* 6:1503–1517.
- Sapir, A., R. Schweitzer, and B. Z. Shilo. 1998. Sequential activation of the EGF receptor pathway during *Drosophila* oogenesis establishes the dorsoventral axis. *Development*. 125:191–200.
- Sauer, H., R. Stanelle, J. Hescheler, and M. Wartenberg. 2002. The DC electrical-field-induced  $\text{Ca}^{2+}$  response and growth stimulation of multicellular tumor spheroids are mediated by ATP release and purinergic receptor stimulation. *J. Cell Sci.* 115:3265–3273.
- Scemes, E., S. O. Suadicani, and D. C. Spray. 2000. Intercellular communication in spinal cord astrocytes: fine tuning between gap junctions and P2 nucleotide receptors in calcium wave propagation. *J. Neurosci.* 20:1435–1445.
- Schlessinger, J. 2000. Cell signaling by receptor tyrosine kinases. *Cell*. 103:211–225.
- Schoeberl, B., C. Eichler-Jonsson, E. D. Gilles, and G. Muller. 2002. Computational modeling of the dynamics of the MAP kinase cascade activated by surface and internalized EGF receptors. *Nat. Biotechnol.* 20:370–375.
- Schuster, S., M. Marhl, and T. Hofer. 2002. Modelling of simple and complex calcium oscillations. From single-cell responses to intercellular signalling. *Eur. J. Biochem.* 269:1333–1355.
- Shiga, H., T. Tojima, and E. Ito. 2001.  $\text{Ca}^{2+}$  signaling regulated by an ATP-dependent autocrine mechanism in astrocytes. *Neuroreport*. 12:2619–2622.
- Shvartsman, S. Y., M. P. Hagan, A. Yacoub, P. Dent, H. S. Wiley, and D. A. Lauffenburger. 2002. Autocrine loops with positive feedback enable context-dependent cell signaling. *Am. J. Physiol. Cell Physiol.* 282:C545–C549.
- Shvartsman, S. Y., H. S. Wiley, W. M. Deen, and D. A. Lauffenburger. 2001. Spatial range of autocrine signaling: modeling and computational analysis. *Biophys. J.* 81:1854–1867.
- Sneyd, J., M. Wilkins, A. Strahonja, and M. J. Sanderson. 1998. Calcium waves and oscillations driven by an intercellular gradient of inositol (1,4,5)-trisphosphate. *Biophys. Chem.* 72:101–109.

- Sommeijer, B. P., L. F. Shampine, and J. G. Verwer. 1998. RKC: An explicit solver for parabolic PDEs. *J. Comput. Appl. Math.* 88:315–326.
- Spradling, A. C. 1993. Developmental Genetics of Oogenesis. The Development of *Drosophila Melanogaster*. Cold Spring Harbor Laboratory Press, Plainview, New York. pp1–70.
- Stemerink, C., and J. Jacobs. 1997. Argos and Spitz group genes function to regulate midline glial cell number in *Drosophila* embryos. *Development*. 124:3787–3796.
- Stevens, L. 1998. Twin Peaks: Spitz and Argos star in patterning of the *Drosophila* embryo. *Cell*. 95:291–294.
- Sturtevant, M. A., J. W. O'Neill, and E. Bier. 1994. Down-regulation of *Drosophila* Egf-r mRNA levels following hyperactivated receptor signaling. *Development*. 120:2593–2600.
- Sunnarborg, S. W., C. L. Hinkle, M. Stevenson, W. E. Russell, C. S. Raska, J. J. Peschon, B. J. Castner, M. J. Gerhart, R. J. Paxton, R. A. Black, and D. Lee. 2002. Tumor necrosis factor- $\alpha$  converting enzyme (TACE) regulates epidermal growth factor receptor ligand availability. *J. Biol. Chem.* 277:12838–12845.
- Tabata, T. 2001. Genetics of morphogen gradients. *Nat. Rev. Genet.* 2: 620–630.
- Tang, Y., and H. G. Othmer. 1995. Excitation, oscillations and wave propagation in a G-protein-based model of signal transduction in *Dictyostelium discoideum*. *Philos. Trans. R. Soc. Lond. B Biol. Sci.* 349:179–195.
- Tang, Y., J. L. Stephenson, and H. G. Othmer. 1996. Simplification and analysis of models of calcium dynamics based on IP3-sensitive calcium channel kinetics. *Biophys. J.* 70:246–263.
- Umata, T., M. Hirata, T. Takahashi, F. Ryu, S. Shida, Y. Takahashi, M. Tsuneoka, Y. Miura, M. Masuda, Y. Horiguchi, and E. Mekada. 2001. A dual signaling cascade that regulates the ectodomain shedding of heparin-binding epidermal growth factor-like growth factor. *J. Biol. Chem.* 276:30475–30482.
- Urban, S., J. R. Lee, and M. Freeman. 2002. A family of Rhomboid intramembrane proteases activates all *Drosophila* membrane-tethered EGF ligands. *EMBO J.* 21:4277–4286.
- Wasserman, J. D., and M. Freeman. 1998. An autoregulatory cascade of EGF receptor signaling patterns the *Drosophila* egg. *Cell*. 95:355–364.
- Waterman, H., and Y. Yarden. 2001. Molecular mechanisms underlying endocytosis and sorting of ErbB receptor tyrosine kinases. *FEBS Lett.* 275:142–152.
- Wiley, H., and P. Burke. 2001. Regulation of receptor tyrosine kinase signaling by endocytic trafficking. *Traffic*. 2:13–18.
- Wiley, H. S., J. J. Herbst, B. Walsh, D. A. Lauffenburger, M. G. Rosenfeld, and G. Gill. 1991. The role of tyrosine kinase activity in endocytosis, compartmentation, and downregulation of the epidermal growth factor receptor. *J. Biol. Chem.* 266:11083–11094.
- Wong, E. S., C. W. Fong, J. Lim, P. Yusoff, B. C. Low, W. Y. Langdon, and G. R. Guy. 2002. Sprouty2 attenuates epidermal growth factor receptor ubiquitylation and endocytosis, and consequently enhances Ras/ERK signalling. *EMBO J.* 21:4796–4808.
- Yan, Y., K. Shirakabe, and Z. Werb. 2002. The metalloprotease Kuzbanian (ADAM10) mediates the transactivation of EGF receptor by G-protein-coupled receptors. *J. Cell Biol.* 158:221–226.
- Zhang, Z., P. Oliver, S. R. Lancaster, P. O. Schwarzenberger, M. S. Joshi, J. Cork, and J. K. Kolls. 2001. Reactive oxygen species mediate tumor necrosis factor  $\alpha$ -converting, enzyme-dependent ectodomain shedding induced by phorbol myristate acetate. *FASEB J.* 15:303–305.